CFD-BASED ANALYSIS OF TURBULENT FLOW AROUND CYLINDRICAL PIERS IN TANDEM ARRANGEMENT

Asif Bin Ferdous[1], Md. Samiun Basir[*2] and Md. Rimon Azad[3]

[1] *Student, Chittagong University of Engineering and Technology, Bangladesh, e-mail: asifb336@gmail.com*
[2] *Assistant Professor, Chittagong University of Engineering and Technology, Bangladesh, e-mail: msbasirwre@cuet.ac.bd*
[3] *Student, Chittagong University of Engineering and Technology, Bangladesh, e-mail: azadrimon24@gmail.com*

***Corresponding Author**

ABSTRACT

This study focuses on the mathematical investigation of turbulent flow around tandem cylindrical piers using computational fluid dynamics (CFD). The setup and essential parameters of the study was based on an existing experimental study performed in a laboratory setting. In the setup, two identical cylindrical piers were positioned along the centerline of a rectangular open channel flume at center-to-center spacings of 3D, 6D, and 9D, where D represents the pier diameter. A three-dimensional CFD model was developed to replicate the conditions of the physical experiment. Simulations were carried out using two industry-standard CFD solvers: Ansys CFX and Ansys Fluent. The computational domain consisted of an 11 m long, 0.76 m wide flume with a uniform flow depth of 0.265 m. Two vertical pier geometries of 0.15 m diameter and 0.265 m height were placed within the flume. A steady inlet velocity of 0.34 m/s was applied, and data were extracted along the symmetry plane of the domain to evaluate velocity and turbulence distributions. Results indicated that Ansys CFX produced velocity profiles that aligned more closely with experimental observations, while turbulence data from Ansys Fluent showed slightly better convergence. The study also revealed that the downstream pier significantly influenced the wake structure in the midstream region. Moreover, the extent of the far wake increased with greater spacing between the piers. These findings provide insight into the hydrodynamic interactions in tandem pier configurations and highlight the applicability of CFD tools in analyzing complex turbulent flow behavior. The comparative evaluation of CFD solvers enhances understanding of their performance in replicating experimental flow characteristics.

Keywords: *Tandem Cylindrical Piers, Turbulent Flow, Computational Fluid Dynamics (CFD), ANSYS CFX and Fluent, Wake Interaction*

1. INTRODUCTION

In order to support transportation networks, bridges are structural components built spanning rivers, lakes, or the ocean (Tang & Puspasari, 2021). The piers that make up bridges primarily restrict the flow pattern and create turbulence characteristics. Bridges are made of round curved piers built over rivers that obstruct fluid movement. For small and medium-sized rivers, many nations, including Bangladesh, construct bridges over oblong piers that serve as bluff bodies (M. S. Basir, 2022; Nowrin, 2020). When constructing bridges and piers, the effects of fluid movement must be taken into consideration, particularly in regions with high water levels or strong currents. In addition to obstructing water flow and causing significant structural damage, turbulent flow around bridge piers can worsen erosion next to those foundations. Therefore, it is crucial to comprehend the turbulent flow characteristics close to bridge piers, which are in charge of scour development, in order to guarantee the security and longevity of these structures (Basir et al. 2022). Studying turbulent flow characteristics over tandem configurations of circular, rectangular, or oblong-shaped piers has drawn more attention in the past few years. The local scour surrounding bridge piers with both circular and non-circular geometry has been the subject of various research (Graf & Istiarto, 2010; Obeid & Al-Shukur, 2016). Because of wake interference between the upstream and downstream structures, the flow field surrounding tandem piers is significantly more complicated than that surrounding a single pier. The pressure distribution, turbulence characteristics, and flow reattachment at the downstream pier are directly impacted by the wake created by the upstream pier, which has large vortices and velocity deficits. These wakes interact to produce extremely three-dimensional, unstable flow patterns with secondary flow structures and high turbulence kinetic energy (TKE). Particularly in the vicinity of the downstream pier, these interactions may expedite scour processes and raise local bed shear stress (Bento et al., 2021; Faheem Sadeque et al., 2009). In many engineering projects (such as bridge piers, offshore and onshore structures, fish habitat structures, etc.), group piers in tandem configurations (in line with the flow) are becoming increasingly common for financial and geotechnical considerations (Ataie-Ashtiani & Aslani-Kordkandi, 2013).

Ansys CFX & Ansys Fluent are CFD platforms that provide strong capabilities for simulating turbulent, free-surface, and incompressible flows utilizing sophisticated numerical techniques (Qi et al., 2020). It is appropriate for assessing the unsteady wake and turbulence behavior related to tandem piers because of its high-accuracy solver and versatile turbulence model option (e.g., k-ε, k-ω SST, Reynolds Stress Model). Researchers can examine how various pier configurations, spacing ratios, and flow conditions affect vortex shedding, flow interference, and turbulent kinetic energy distributions by simulating these variables using Ansys CFX & Fluent (Hashemi et al., 2019; Malik & Setia, 2020). Additionally, some studies on flow around single circular cylinders have used a 2D numerical model to demonstrate wakes behind a circular cylinder, although the model is inadequate and cannot yield correct results due to parameterization. Since bridge piers are typically built for double pile-like cylindrical piers, it is important to evaluate the flow around double pile-like tandem piers at the laboratory scale in order to enhance bridge design parameters and validate in Ansys CFX & Fluent Model.

2. METHODOLOGY

2.1 Pre-model Setup

The setup of the mathematical model was established in reference to a real-world laboratory experiment as orchestrated by Zobeyer et al., 2021. The laboratory experiment was described to be conducted in a rectangular recirculating flume of 21.3 m length, 0.76 m height and 0.74 m depth with a longitudinal bed slope of 1.87×10^{-3}. Two circular cylinders of concrete material were placed as flow obstruction objects to represent piers. The cylinders were assembled with uniform dimensions of 0.30 m height and 0.15 m diameter and arranged in tandem towards the direction of the flow, and the first cylinder was placed at 11.0 m from the inlet. The laboratory setup was reproduced as a fluid domain

for CFD simulation. To minimize the high computational requirement that would potentially outpower the available computational setup, the length of the flume and the placement of the first pier were reduced in the CFD setup while ensuring critical parameters like flow development, data collection sections and wake zone expansion to be uninterrupted in the process. Since only the fluid domain was designed, flume and pier height were reduced to match the flow height (0.265 m). Table 1 provides a brief description of the contrasted dimensions.

Table 1: Scaling of laboratory experiment vs mathematical model

Variable	Laboratory Experiment	Mathematical Model
Length of flume	21.3 m	11.0 m
Width of flume	0.76 m	0.76 m
Depth of flume	0.74 m	0.265 m
Height of cylinder. h	0.30 m	0.265 m
Diameter of cylinder, D	0.15 m	0.15 m
Distance of first cylinder from inlet	11.0 m	6.0 m

The first cylinder from the inlet was defined as 'upstream pier' followed by the 'downstream pier' in its wake. The experimental setups were diversified by the variable placement of downstream pier relative to the position of the upstream pier. Thus, three different experimental cases were developed for the respective gap ratios of L/D = 3D (Case-1), L/D = 6D (Case-2) and L/D = 9D (Case-3) centre-to-centre (c/c) spacing between the piers. The cases are abbreviated as C1, C2 and C3 respectively. The region between the two piers was defined as 'midstream region' and that beyond the downstream pier as 'downstream region'. Data collection sections were defined in these regions along the symmetrical plane of the flume as shown in Figure 1. Each collection section comprised 11 data observation points vertically along the depth of the flume.

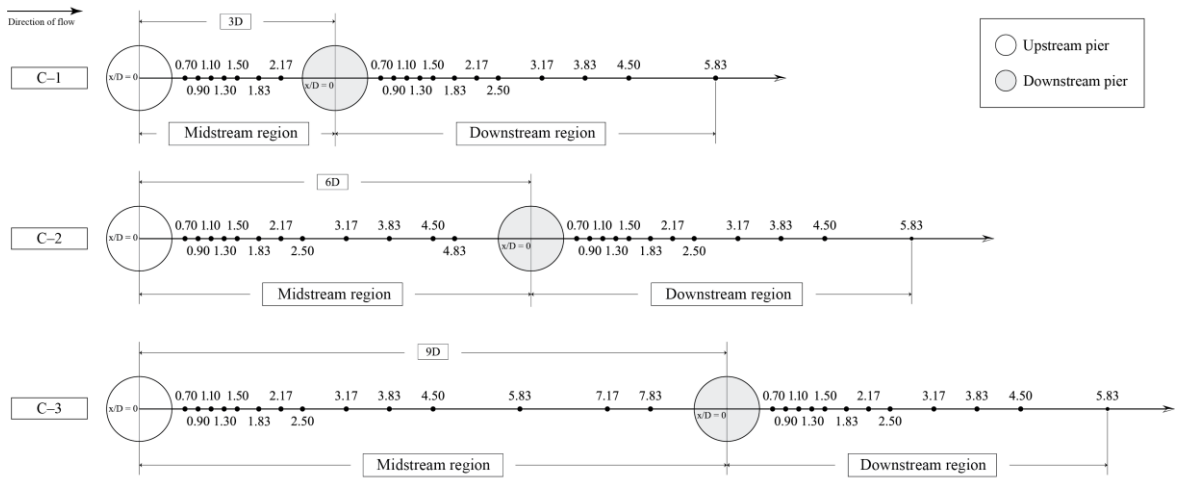

Figure 1: Plan view of data collection sections

Key experimental parameters were calculated as shown in Table 2.

Table 2: Calculation of experimental parameters

Discharge (m^3/s)	Width of Flume (m)	Water depth, H (m)	Cross-sectional Mean Velocity, U_o (m^3/s)	Kinematic Viscosity of water, U (m^2/s)	Froud Number, F	Reynolds number, R
0.069	0.76	0.265	0.34	1×10^{-6}	0.21	52900

2.2 Modeling Workflow

The mathematical model was accomplished with three-dimensional CFD modeling workflow. Two CFD software - Ansys CFX and Ansys Fluent were used in the process. CFD modeling involves three principal steps - preprocessing, processing and post-processing, each of which are covered by both the software's readily available toolsets. With three case setups replicating in both software, a total of 6 experimental runs were conducted as shown in Table 3.

Table 3: Experimental runs

Run no.	Case	Pier spacing	Software
1	1	3D	Ansys CFX
2	2	6D	
3	3	9D	
4	1	3D	Ansys Fluent
5	2	6D	
6	3	9D	

In the preprocessing step, common scene geometries were designed with Ansys Design Modeler, and an unstructured tetrahedral mesh with cell size ranging from 0.005 m to 0.015 was applied. In the processing step, Shear Stress Transport (SST K-ω) was given as the turbulence model for both CFX and Fluent setups. As for boundary conditions, 0.34 m/s was selected as the inlet velocity in the beginning face and 'Outlet' was selected at the end face of the fluid domain. The side and bottom walls were defined as 'No Slip wall'. The models did not use any free surface model. In CFX, the top wall was selected as 'Free Slip Wall' to simulate a dynamic water surface behavior. In Fluent, however, since no other options provided with more satisfactory simulation results, the top wall was selected as 'No Slip Wall' which might have potentially reduced the numerical accuracy in the observation points near the water surface. Both the models were performed as transient (time-dependent) solution and were run for a total of 120 s time with 1 s time-step size. To achieve numerical stability of the solutions, convergence criteria were given 1×10^{-6} for the governing equations and the number of iterations for timesteps was set to 30 for CFX and 50 for Fluent. After the setup configuration was done, simulation was started.

Finally, post-processing was done in Ansys CFD-Post for both models. By using probe function, point data for each observation points at all the sections were extracted for longitudinal velocity and TKE. The extracted datasets were collected in a spreadsheet software for further processing and visualization.

3. RESULTS AND DISCUSSION

The study attempted to numerically capture the dynamic response of mean flow to varying streamwise distances between tandem piers using Ansys Fluent and Ansys CFX in contrast to their laboratory counterpart. Velocity and turbulence were used as the measuring metrics. For velocity, the x-directional component in the streamwise direction was considered and thus termed as longitudinal velocity (u). Turbulence was measured in terms of turbulent kinetic energy (TKE). Both variables can be directly obtained using 'Ansys-Post' post-processing software provided by Ansys. The obtained numerical values of u and TKE were normalized using the mean velocity, U_o as u/U_o and KE/U_o^2, respectively to be represented as dimensionless while visualizing. The streamwise distances were normalized as x/D, where x was the location of corresponding data collection section as referenced in Figure 1, D being the pier diameter. The vertical distances at each section were normalized as z/H, z representing the vertical distances of data collection point and H the depth of flow.

All the necessary data were collected with sufficient spatial frequency as schemed in Figure 1; however, visualizing for each section separately would be massively spacious. Hence, rather than mass representation, key sections were selected for visualizing the findings within optimum plotting scope.

3.1 Velocity Insights

Figure 2 and Figure 3 show the vertical profiles of longitudinal velocity in the selected stations for C1, C2 and C3 cases as modelled in CFX and Fluent respectively. Preliminary observations reveal that the profiles from CFX possess qualitatively more defined and regulated patterns than those from Fluent. Fluent patterns, on the other hand, show a slightly wider numerical variation in the positive x-axis. Figure 4 and Figure 5 feature the contours of longitudinal velocity in the wake zone as derived from the models, CFX and Fluent, respectively. On comparison, CFX velocity patterns appear to show better wake definition as usual.

3.1.1 Longitudinal Velocity Profiles

Figure 2(a), in the midstream, longitudinal velocities from CFX are mostly negative just immediate to the upstream pier at x/D = 0.70 section for all three cases. The numerical values of longitudinal velocity start negative near the channel bed, gradually encroaches the positive axis at mid-height and makes a return for the negative as water surface is approached. Despite some interference with the positive axis, reverse velocities dominate the vertical flow profile at this section suggesting the formation of a near wake zone. This is followed by an overall increase in velocity as the flow advances further from the upstream pier. Numerical velocities start negative near the channel bed at x/D = 1.83 for each of the cases, however, they show a strong bias to the positive axis towards mid-height and a decrease within the positive axis is followed up until near the water surface, indicating a gradual recovery of flow in progression. Flow velocities past x/D = 2 show rather stable vertical patterns in C2 and C3 cases. Remarkably, at x/D = 4.50, velocities range smaller in C2 than those from C3, underlining the effect of closer downstream pier placement on flow recovery in the former case.

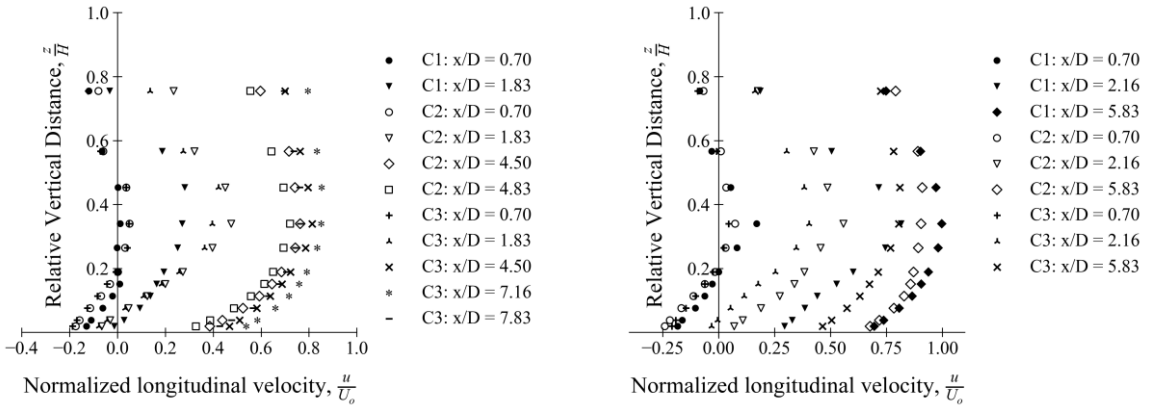

(a) (b)

Figure 2: Longitudinal velocity profiles from Ansys CFX at selected stations (a) in midstream (b) in downstream

Observations from Figure 2(b) reveals similar findings at x/D = 0.70 and beyond for all three cases at downstream, i.e. velocities starting negative and consequently showing a gradual shift from negative axis to positive as flow progresses away from the downstream pier. However, velocities at x/D = 5.83 range highest to lowest from C1 to C3, indicating that flow past downstream pier show a rather speedy recovery in case of closer c/c pier placement.

Velocity profiles from Fluent as illustrated in Figure 3 correspond to the same data collection locations with different patterns. In both upstream and downstream cases, velocities can be seen

mostly positive. In Figure 3(a), in C1 and C2 cases of the midstream region, flow near the channel bed at x/D = 0.70 shows negative velocities, which is followed by a relatively faster increase towards the positive axis with increase in z/H height. In C3 case, velocities can be seen positive throughout the flow depth. However, the usual pattern of increase in velocity with height is still present. With increase in x/D distances, velocities can be seen regaining positive magnitudes as expected.

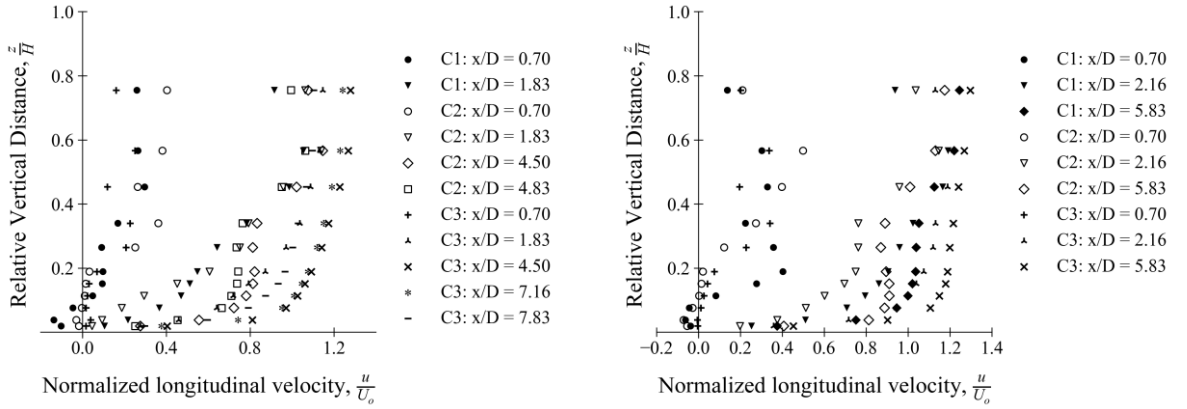

(a) (b)

Figure 3: Longitudinal velocity profiles from Ansys Fluent at selected stations (a) in midstream (b) in downstream

In Figure 3(b), at x/D = 0.70 in the downstream region, velocities near the channel bed can be seen negative in all cases, with stronger appearances made in the cases C1 and C2 than that in C3. With increase in distance from the downstream pier (x/D > 2), velocities across the flow depth show increase in positive magnitudes as expected, leading to gradual development of more stable profiles, indicating a recovery of flow in the far wake.

3.1.2 Longitudinal Velocity Contours

Figure 4 features the contour profiles of longitudinal velocity from CFX model on the plane of symmetry along the centerline of the flume. From C1 to C3, the maximum velocity can be seen increasing with increase in pier spacing in the midstream region starting with $u/U_o > 0.15$ in C1, reaching approximately $u/U_o = 0.75$ in C2 and exceeds $u/U_o > 0.75$ in C3. This increase suggests that the midstream wake flow successively expands due to the placement of downstream pier at further distances which introduces more spatial span to regain the regular flow momentum, thus develop far wake flow with decreased turbulence. The near wake flow, which is characterized by a presence of reverse velocity vectors and chaotic vertical profiles, can be seen approximately up to x/D = 1.9 in C1, and x/D = 2 in C2 and C3 cases, indicating that near wake flow zone also increases with increased pier spacing.

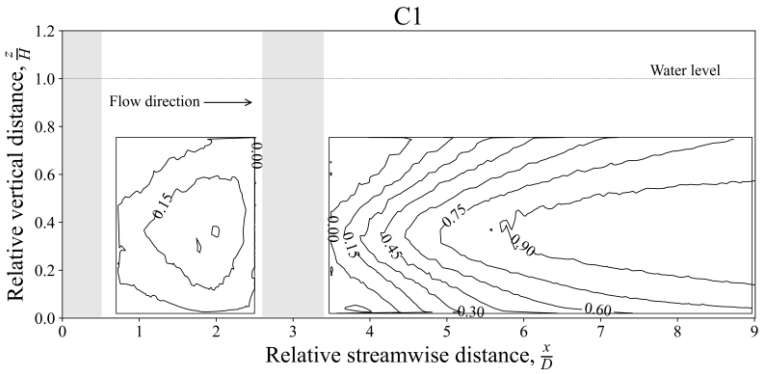

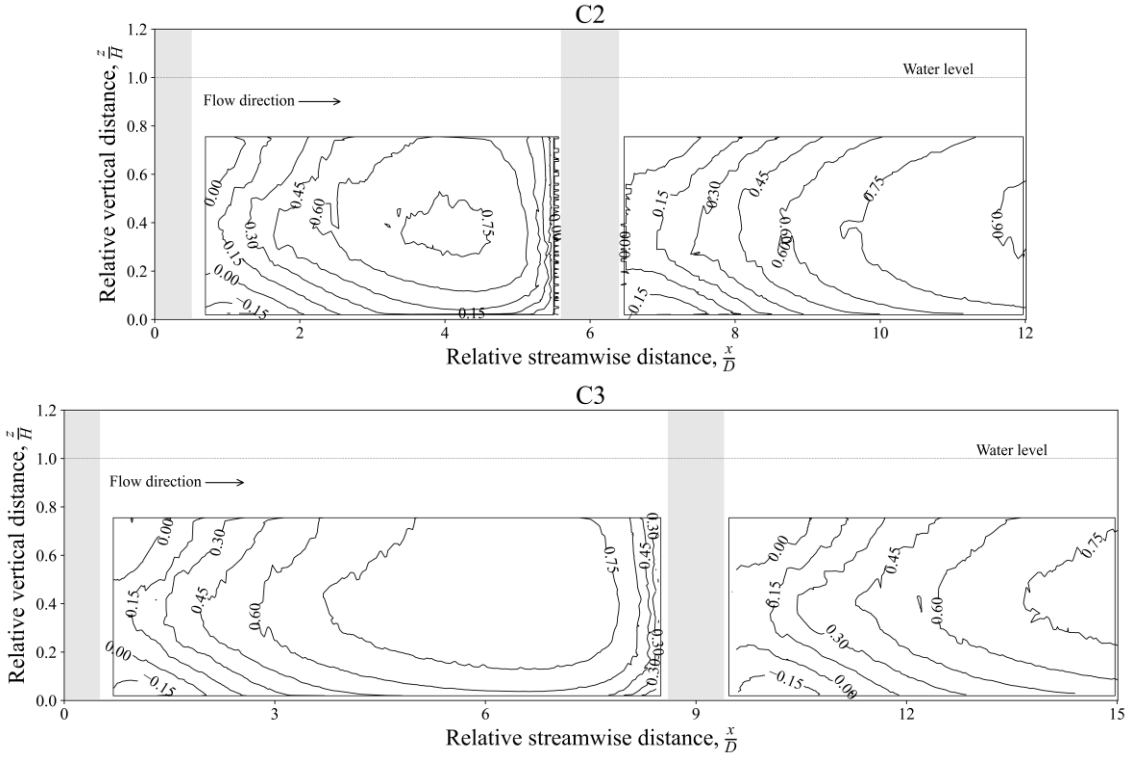

Figure 4: Contours of normalized longitudinal velocity (Ansys CFX)

Figure 5 defines the contour profiles of longitudinal velocity from Fluent model in the same location as CFX. Upon quick visual inspection, however, it appears that the resultant profiles are relatively less ideal in this model. The maximum velocities in the midstream region show the usual increase from C1 to C3; $u/U_o = 1.0$ in C1, $u/U_o > 1.0$ in C2 and $u/U_o = 1.2$ in C3, implying the enlargement of far wake zone with growing pier spaces. Near wake flow can be seen up to $x/D = 1.2$ in C1 and $x/D = 1.3$ in C2. In C3, the presence of reverse velocities is insignificant with their expansion within $x/D < 1$, which puts this case in contrast to the same case from Fluent.

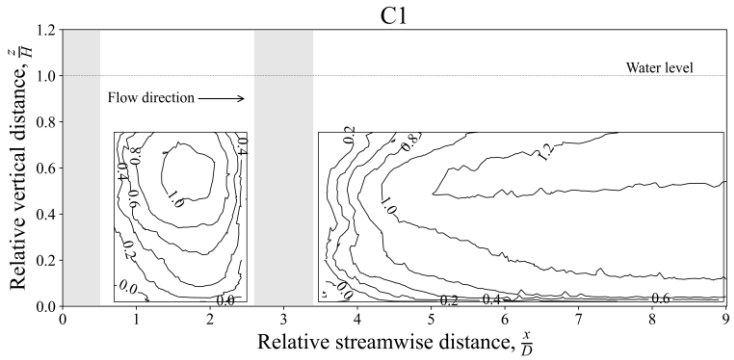

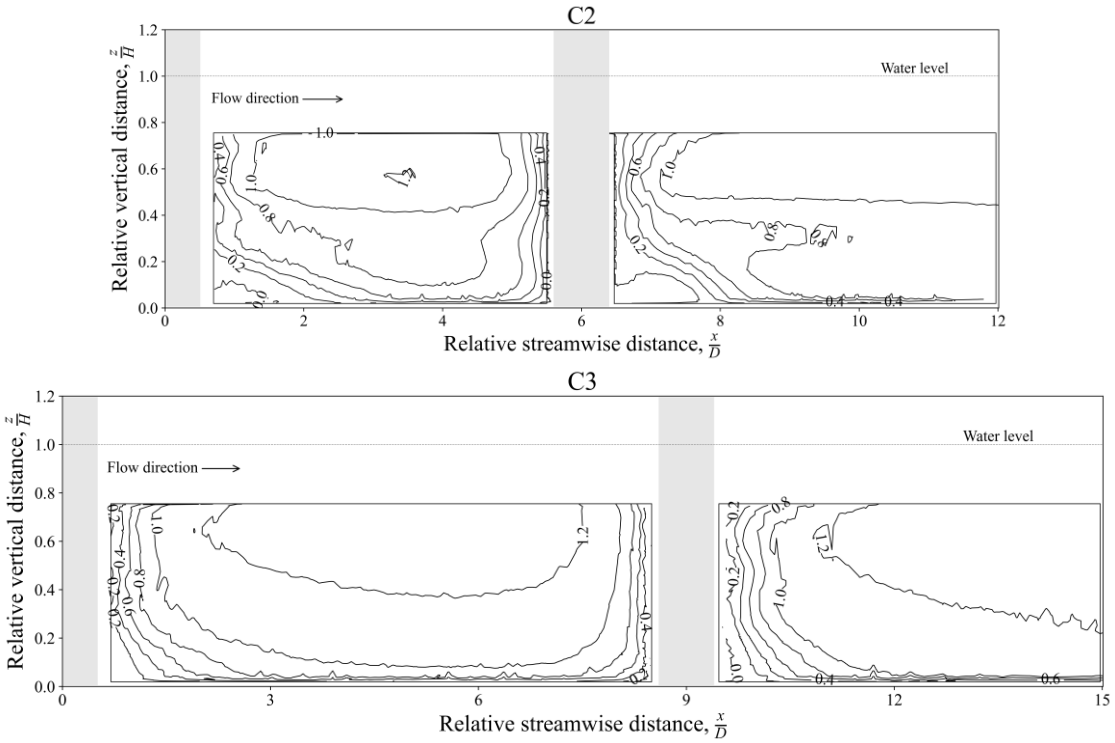

Figure 5: Contours of normalized longitudinal velocity (Ansys Fluent)

3.2 Turbulence Insights

Figure 6 and Figure 7 present the vertical profiles of normalized turbulent kinetic energy (TKE) at the selected stations from CFX and Fluent, respectively. In general, TKE profiles show an overall increase from channel bed to the water surface in CFX and an overall decrease (not necessarily) in Fluent results.

Close inspection of midstream profiles from all the CFX cases in Figure 6(a) reveals that at x/D = 0.7, TKE do not vary much in terms of magnitude and pattern from channel bed to near the water surface, which suggests the emergent turbulence is not affected much by the downstream pier. However, at sections near the end of the midstream regions in C1 (x/D = 1.83), C2 (x/D = 4.83) and C3 (x/D = 7.83), TKE magnitudes vary by great differences, with C1 outnumbering the rest of the cases followed by C2. The farther placement of the downstream pier provides more scope for regaining flow momentum, thus a reduction in turbulence magnitudes in the last sections of C2 and C3 following an increase in the intermediate sections with an advancement in pier distance is just as expected. A similar variability with increase in pier spacing can be noted in the downstream case (Figure 6(b)), where the only exception is the decreased magnitudes from the last section in C1 case, which is as expected given the endless flow development scope in the wake of the downstream pier.

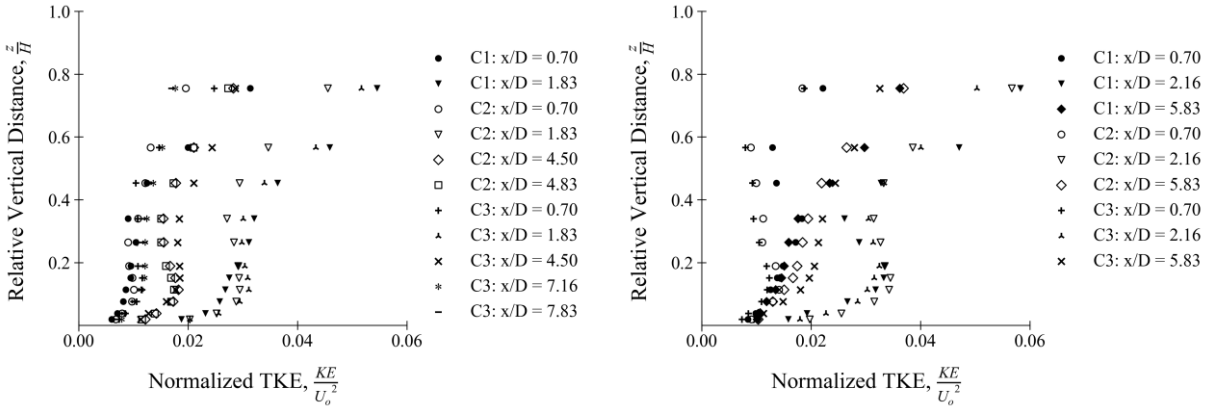

(a) (b)

Figure 6: Normalized TKE profiles from Ansys CFX at selected stations (a) in midstream (b) in downstream

In the Fluent midstream cases in Figure 7(a), while TKE magnitudes from different cases at x/D = 0.70 are at proximity to some degree, their vertical patterns show irregular differences. With increasing pier spacing, the last section in the respective cases show decrease in magnitude as usual, however, the patterns are chaotic and overlaps of vertical profiles from different sections of the same cases occur. In the downstream, the usual patterns of increase in TKE magnitudes in the second selected section followed by a decrease in the last section can be noted. Overlaps also occur in this region to some extent.

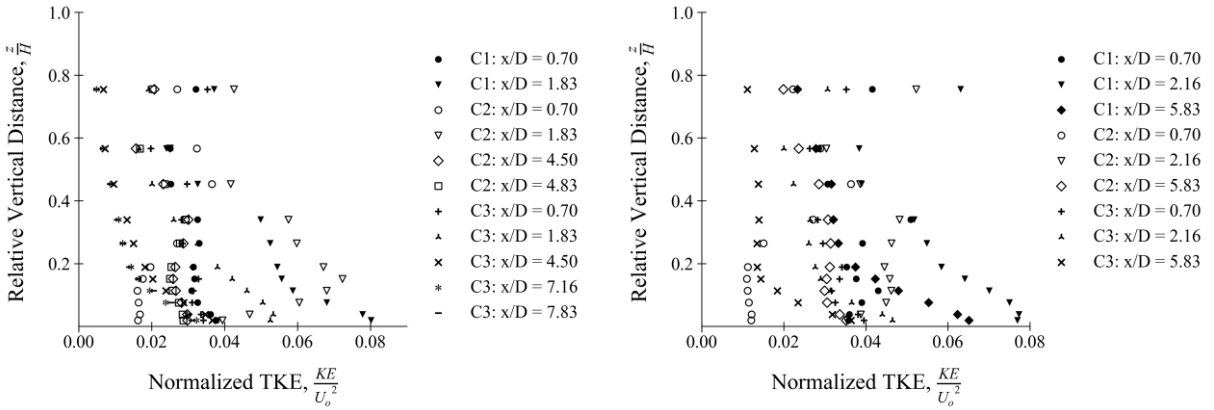

(a) (b)

Figure 7: Normalized TKE profiles from Ansys Fluent at selected stations (a) in midstream (b) in downstream

3.3 Comparison

Figure 8 and Figure 9 feature comparative illustrations of data from the CFD models and the laboratory experiment for normalized velocity and TKE, respectively in the selected sections.

In Figure 8, for all regions in different cases, it is apparent that CFX offers superior convergence to experimental velocity data than Fluent. While the velocity profiles in the first section from the laboratory experiment are mostly in the reverse zone, the CFX velocities are reverse mostly near the channel bed and the water surface with more streamlined profiles. However, later sections converge more in terms of magnitude and pattern. On the other hand, Fluent profiles diverge relatively towards the higher ranges for the same sections, putting its results in contrast to those from CFX.

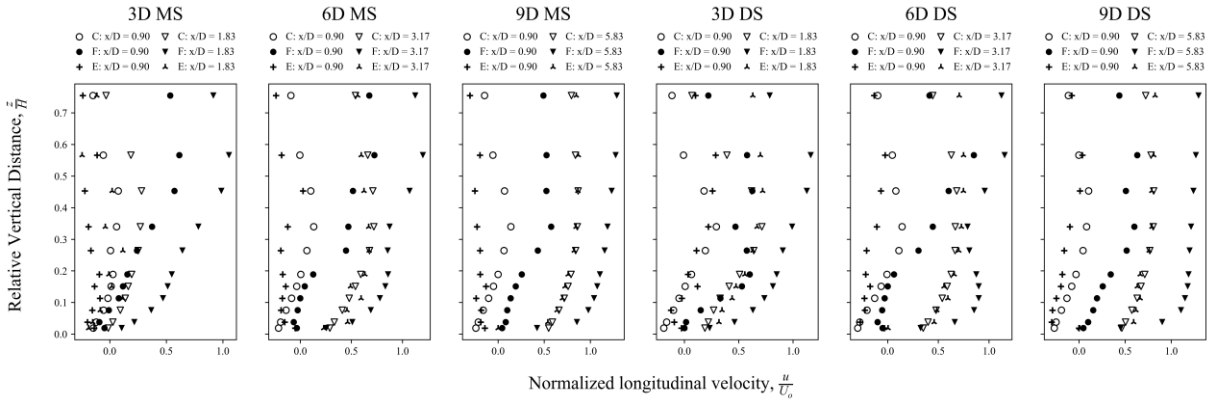

Figure 8: Comparison of velocity profiles between CFX (C), Fluent (F) and laboratory experiment (E)

In Figure 9, in all the regions for all cases, TKE profiles from both CFX and Fluent show relatively higher divergence from the experimental profiles. The difference can be seen in the respective patterns as well. However, Fluent-derived profiles have higher TKE magnitudes than CFX, putting them relatively closer to the experimental results. The choice of turbulence model and their in-model configurations can be the primary influencing factor.

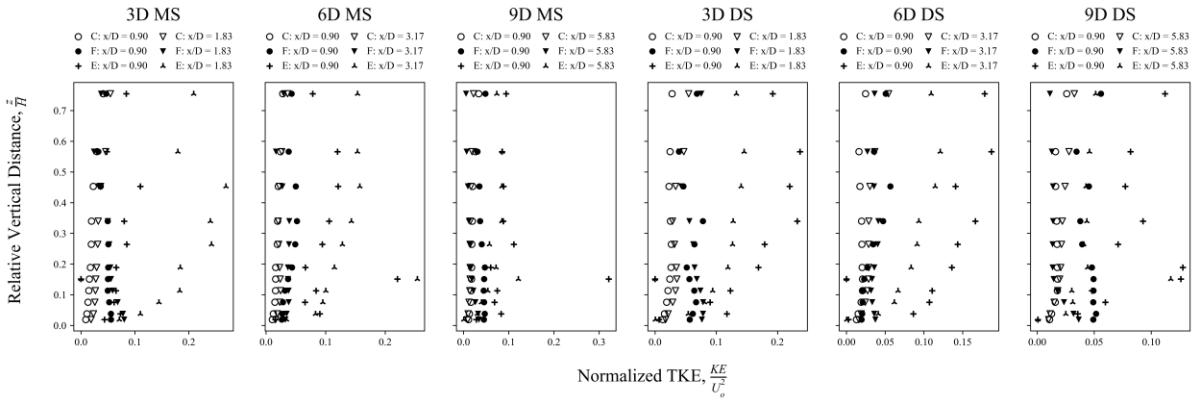

Figure 9: Comparison of TKE profiles between CFX (C), Fluent (F) and laboratory experiment (E)

Overall assessment is such that, in terms of velocity, CFX provides satisfactory convergence to laboratory data than Fluent. On the other hand, in terms of TKE, while Fluent results show a bit closer proximity to the laboratory data, neither model provided satisfactory convergence.

4. CONCLUSIONS

This study focused on investigating the emergence and expansion of turbulent flow around tandem piers using CFD modeling tools based on a laboratory experiment by Zobeyer et al. Ansys CFX and Fluent were used to conduct the experiment. The processing step has been different in either of the software due to difference in software architecture, yet similarity in terms of model configuration were attempted to achieve with some minor discrepancies. The results, however, for the applied configurations have been remarkably different, highlighting different strength of areas for either of the software. The experiment underlines some important findings regarding flow behavior in the wake of cylindrical shaped piers, its dynamic response to changing c/c spacing of tandem piers and the applicability of CFD in such studies.

- The placement of a second (downstream) pier and its relative distance from the upstream one affects the wake flow in the midstream region.

- An increase in c/c spacing between the tandem piers lead to an expansion of emergent wake flow in the midstream region, driving the far wake farther away.
- Different pier spacing affects wake flow in the downstream region as well, influencing flow turbulence and its expansion in the region.
- The pier spacing also dictates the spatial development of flow in the far wake zone for both midstream and downstream.
- The wake patterns, velocity and turbulence profiles made superior appearances in CFX model than those from Fluent model for the given configurations.
- When compared with laboratory experiment, CFX shows better representability of the laboratory experiment compared to Fluent for the given configurations.
- In terms of longitudinal velocity, CFX provides better convergence to experimental results while Fluent results show some degree of divergence.
- In terms of TKE, while the results from the models show some convergence in comparison to each other, either of them demonstrates poorer convergence to laboratory experiment results in terms of magnitudes.

For the tested configurations, Ansys CFX appears to offer better utility for studying turbulence flow around tandem pier setup. However, Ansys Fluent can also be potentially improved with better combination of configuration and model setup, by refining to granules with numerous trial-and-error experiments. The methodology is recommended to further enhance for both of the models by introducing free surface modeling and complex air-water interactions, different types of sediments in the bed, increasing mesh resolution to finer degrees for higher cell counts, examining with more calculation-intensive turbulence models of higher counts of governing equations and performing corresponding CFD calculations in a strong computer machine.

DECLARATION OF USE OF AI

ChatGPT (chatgpt.com) was employed to support the expansion and refinement of the core research topic, as well as to facilitate a clearer understanding of fundamental concepts and key terminology that underpin the study. Relevant associated concepts were also critically reviewed using this tool. Furthermore, ChatGPT (chatgpt.com) and the AI-powered paraphrasing tool QuillBot (quillbot.com) were utilized to revise and enhance selected sections of the manuscript and to paraphrase essential quotations from pertinent scholarly literature.

REFERENCES

Ataie-Ashtiani, B., & Aslani-Kordkandi, A. (2013). Flow field around single and tandem piers. *Flow, Turbulence and Combustion*, *90*(3), 471–490.

Basir, M. S. (2022). *Experimental Investigation of Local Scour Around Two Cylinder-Shaped Piers in Tandem Arrangements*. M.Sc. Thesis. Bangladesh University of Engineering and Technology. Dhaka-1000.

Basir, M. S. ; I. M. M. ; M. B. (2022). Experimental Investigation of Pier Shape Effect on Local Scour Around Two Tandem Piers. *Proceedings of the 5th Annual Paper Meet & 2nd Civil Engineering Congress*, 428-433.

Bento, A. M., Viseu, T., Pêgo, J. P., & Couto, L. (2021). Experimental characterization of the flow field around oblong bridge piers. *Fluids*, *6*(11).

Faheem Sadeque, M. A., Rajaratnam, N., & Loewen, M. R. (2009). Shallow turbulent wakes behind bed-mounted cylinders in open channels. *Journal of Hydraulic Research*, *47*(6), 727–743.

Graf, W. H., & Istiarto, I. (2010). Flow pattern in the scour hole around a cylinder. *Journal of Hydraulic Research*, *40*(1), 13–20.

Hashemi, M., Zomorodian, M. A., & Alishahi, M. M. (2019). Simulation of Turbulent Flow Around Tandem Piers. *Iranian Journal of Science and Technology - Transactions of Civil Engineering*, *43*(4), 761–768.

Malik, R., & Setia, B. (2020). Interference between pier models and its effects on scour depth. *SN Applied Sciences*, *2*(1).

Nowrin, S. N. (2020). *Experimental Study on Turbulent Flow around a Pair of Cylinders Placed along Plane of Symmetry in a Rectangular Open Channel*. M.Sc Thesis. Bangladesh University of Engineering and Technology, Dhaka-1000.

Obeid, Z. H., & Al-Shukur, A.-H. K. (2016). Experimental Study of Bridge Pier Shape to Minimize Local Scour. *International Journal of Civil Engineering and Technology*, *7*(1), 162–171.

Qi, H., Zheng, J., & Zhang, C. (2020). Numerical simulation of velocity field around two columns of tandem piers of the longitudinal bridge. *Fluids*, *5*(1).

Tang, J. H., & Puspasari, A. D. (2021). Numerical simulation of local scour around three cylindrical piles in a tandem arrangement. *Water (Switzerland)*, *13*(24).

Zobeyer, H., Baki, A. B. M., & Nowrin, S. N. (2021). Interactions between tandem cylinders in an open channel: Impact on mean and turbulent flow characteristics. *Water (Switzerland)*, *13*(13), 1–13.